

## Extreme Starbursts and the Low Mass IMF

Nick Scoville and Gongjie Li

California Institute of Technology, MC 249-17, Pasadena, CA 91125, USA

**Abstract.** The temperatures and densities of the interstellar medium (ISM) in starburst galaxies are greatly elevated compared to those in star forming giant molecular clouds (GMCs) in normal galaxies. I review the observed ISM properties in the prototype starburst Arp 200 and then discuss considerations for star formation in such starburst galaxy nuclei. We have also found a previously unrecognized observational constraint on the low mass star populations applicable to these starbursts. Using stellar population synthesis models from Starburst99 with instantaneous and constant starbursts, we identify and quantify spectral diagnostics for stellar populations. The characteristic age of the stellar population dominating the restframe optical (not the younger stars dominating the UV) can be estimated from the 4000Å break strength (D4000). We find that the presence of the 4000Å break requires a stellar population older than ~100 Myr (since OB stars would dominate the continuum short of 4000Å and they exhibit no break). Very importantly, we also find that the initial mass function (IMF) must extend down to a few solar masses if the 4000Å break is present. Thus, the *detection of the 4000Å break implies an IMF extending to low mass*. The strength of the 4000Å break can be used to constrain the IMF at low stellar masses, while the absence of the feature could be used to identify PopIII stars (which would have low metallicity and probably few low mass stars). The break is, in fact, observed in Arp 220 and in the  $z = 2 - 7$  galaxy SEDs, *casting doubt on recent suggestions of top heavy IMFs for high  $z$  galaxies and starbursts*.

The apparent invariance of the IMF is likely due to the fact that the fragmentation scale for stellar mass condensations occurs at very high density on scales of ~100 AU. At this point, the densities will be  $\sim 10^{11}$  per cc and the initial conditions in the galactic GMCs will have been long forgotten. This 100 AU scale corresponds to the point at which solar mass condensations become optical thick in the far infrared and thus separate quasi-statically from the overall collapse – it is also the typical scale of binary star separations, lending support to the notion that this is the scale for stellar mass fragmentation within collapsing cloud cores.

### 1. Introduction

In starburst galaxies such as the local ultra-luminous infrared galaxies (ULIRGs) and high redshift submm galaxies, the rates of star formation measured relative to the ISM gas supply are elevated by factors of 10 – 100 compared to the average star formation efficiency of a galaxy like the Milky Way. In the local ULIRGs, it is clear that the starbursts are dynamically triggered since they are either merging or post-interacting systems and the ISM is typically highly concentrated in the galactic nuclei. In this

contribution, I summarize what is known of the physical conditions in these starburst systems where the gas can be 5-10 times hotter and 100-1000 times denser than in Galactic giant molecular clouds (GMCs). In the high- $z$  submm galaxies, the physical conditions are less well-constrained but are likely to resemble those in the ULIRGs. Given these extreme differences in both the density and temperature of the ISM, it is natural to expect variations in the initial mass function IMF with perhaps a smaller fraction of low mass stars in the starburst galaxies.

In the past, it has been extremely difficult to constrain the mass of lower mass stars in such galaxies since their luminosity is swamped by the much more luminous OBA-type stars. Here we point out that the 4000Å break feature requires the formation of low mass stars and since this feature is, in fact, seen in these galaxies, they must be forming low mass stars (down to a few  $M_{\odot}$ ).

## 2. The Extreme Starburst – Arp 220 : Lessons for High- $z$ Starbursts ?

Arp 220, at 77 Mpc, is one of the nearest and the best known ultra-luminous merging systems ( $L_{8-1000\mu m} = 1.5 \times 10^{12} L_{\odot}$ ). Visual wavelength images reveal two faint tidal tails, indicating a recent tidal interaction (Joseph & Wright 1985), and high resolution radio and near-infrared imaging show a double nucleus (Baan & Haschick 1995; Scoville et al. 1998). The radio nuclei are separated by 0.98'' at P.A.  $\sim 90^{\circ}$ , corresponding to 350 pc. To power the energy output seen in the infrared by young stars requires a star formation rate of  $\sim 10^2 M_{\odot} \text{ yr}^{-1}$ . The CO (2–1) line emission, mapped at 1'' resolution, showed two peaks separated by 0.9'', and an inclined disk of molecular gas (Scoville et al. 1997; Downes & Solomon 1998). These peaks correspond well with the double nuclei seen in near-infrared and radio continuum images. The 0.5'' resolution CO and 1.3 mm continuum maps obtained by Sakamoto et al. (1999) reveal **counter-rotating** disks of gas in each of the nuclei. The kinematic data clearly require very high mass concentrations in each nucleus, consistent with their being individual galactic nuclei. The masses in each nucleus are apparently dominated by the molecular gas with a gas mass fraction of  $\sim 50\%$  – a common finding of the ULIRG galaxy studies (Bryant & Scoville 1999).

Within each of the Arp 220 nuclei the molecular gas mass is  $\sim 3 \times 10^{10} M_{\odot}$ . The high brightness temperatures of the CO lines (similar to the dust color temperature) implies that the gas in each disk is smoothly distributed rather than be in individual self-gravitating GMCs. The mean density of the gas is  $10^{5-6}$  per cc and the visual extinctions estimated perpendicular to each disk are  $A_V \gtrsim 1000$  mags.

## 3. Black Hole Accretion and Star Formation in the Nuclear ISM

For both Sgr A and Arp 220, which have luminosities differing by over  $10^6$ , the time-averaged accretion rates (obtained from the black hole masses divided by the Hubble time or from the observed luminosities) are orders of magnitude less than the masses of nearby ISM divided by their respective orbital timescales. For the Sgr A\* and Arp 220,  $M_{ISM}/\tau_{orbit} = \text{few } M_{\odot} \text{ per year}$  and  $10^4 M_{\odot} \text{ per year}$ , respectively. Thus it is apparent that: either the fraction of material actually accreted is very small or the accretion timescale is  $\sim 10^4$  orbital periods.

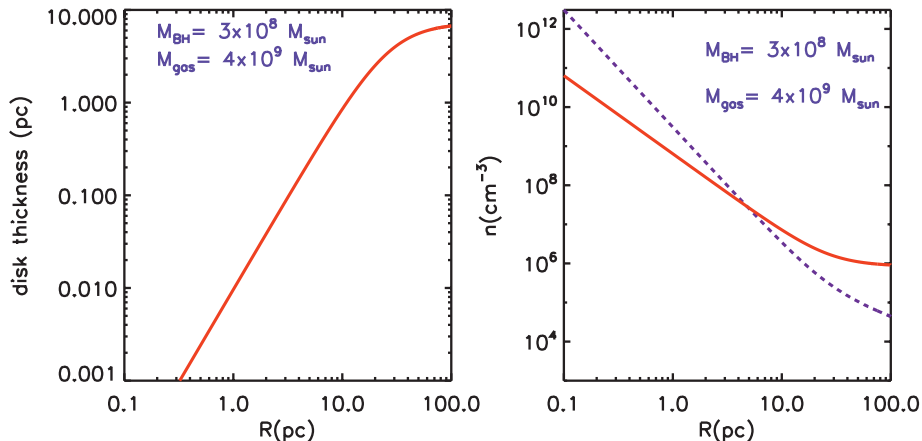


Figure 1. A very crude model for the disk in gas-rich merging systems like Arp 220 is shown. We assume a central point mass (black hole) and a uniform gas surface density disk extending to 100 pc radius. The turbulent velocity dispersion within the disk is taken to be 50 km/s (based on Arp 220; Scoville et al 1997). The disk thickness as a function of radius for hydrostatic equilibrium is shown in the right panel and the mean gas density in the left panel (solid red line). The critical density required for stability of a self-gravitating object (e.g. a cloud) in the disk is shown by the dashed (blue) curve. The right panel shows the extraordinarily high gas densities expected for these very simple assumptions and underscores the fact that self-gravitating clouds should not form in the inner disk due to tidal disruption.

One very effective means of restricting the accretion (or even ejecting the dense ISM) is via the radiation pressure of the AGN acting on the associated dust (Scoville 2003). For a self-gravitating gas and dust mass, the effective ‘Eddington’ limit is approximately  $500 L_{\odot}/M_{\odot}$ , similar to the overall mass-to-light ratio measured in the Arp 220 nucleus ( $10^{12} L_{\odot} / 3 \times 10^9 M_{\odot}$ ). For luminosity-to-mass ratios higher than the ‘Eddington’ limit of  $\sim 500 L_{\odot}/M_{\odot}$  the ISM would be blown out by radiation pressure on the dust.

A similar ‘Eddington’ limit applies for dust embedded starburst regions – the only difference being that the luminosity is from OB stars rather than black hole accretion (Scoville et al. 2001; Scoville 2003; Murray et al. 2005; Thompson et al. 2005). It turns out that large scale nuclear starbursts such as that in Arp 220 have approximately the same empirical limit of  $500 L_{\odot} / M_{\odot}$ , suggesting that nuclear starburst activity may also be regulated by a balance of self-gravity and radiation pressure support.

### 3.1. Nuclear ISM Disk Properties

As a first step, toward understanding the massive gas disks like that seen in Arp 220, we consider an extremely simple model with uniform gas surface density out to radius 100 pc. At the center of the disk, we imagine a point mass of  $4 \times 10^8 M_{\odot}$  – either a central black hole or a nuclear star cluster. The disk is assumed to be self-gravitating and in hydrostatic equilibrium with a sound speed of 50 km/s, representative of the turbulent velocity dispersion measured in Arp 220. Although this is meant only as an

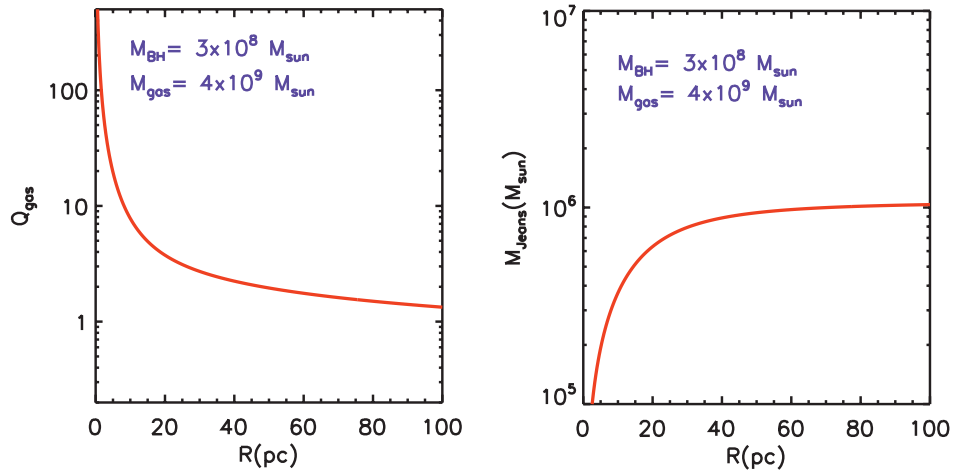


Figure 2. The left panel shows the Toomre  $Q$  stability parameter ( $Q < 1$  unstable) for the disk parameters in Fig. 1; the right panel shows the Jean mass for collapse/self-gravitation assuming a sound speed of 50 km/s and neglecting tidal shear.

illustrative, *gedanken*, experiment, it clearly shows that the conditions are inescapably different from those of star forming clouds in the Galactic disk.

In Figure 1, the disk thickness and mean gas densities are shown as a function of radius out to 100 pc. The thickness of the disk is typically less than 10 pc and the mean densities are everywhere  $> 10^6$ , getting up to  $10^{10} \text{ cm}^{-3}$  near the center. The right panel of Figure 1 also shows the gas density required for tidal stability (dashed line) – clearly demonstrating that it will be difficult to form stable clouds within the central 10 pc radius. Within this region, we should expect a more continuous gaseous disk structure, not a cloudy ISM as found in the center of our Galaxy.

The gravitational stability of the disk can also be seen from the Toomre  $Q$  parameter shown in Figure 2-left. Within the inner 10 pc,  $Q \gg 1$  and it is very hard to form self-gravitating structures in the ISM, such as clouds. On the other hand, outside 10 pc radius such clouds might form (if they are not disrupted by cloud collisions) but their masses are required to be very large, exceeding  $10^6 M_{\odot}$  (Fig. 2-right).

#### 4. Starburst Modeling to Constrain the IMF

To obtain the intrinsic (unextincted) spectra of star forming galaxies, we (Li et al. 2010) have used the Starburst99 galactic spectral synthesis program. Starburst99 makes use of observed Galactic stellar spectra (Vázquez & Leitherer 2005) together with theoretical stellar evolutionary tracks, stellar atmospheres and spectral templates. This updated version of Starburst99 (Vázquez & Leitherer 2005) includes treatment of the thermally pulsing AGB stars which were not included in earlier versions. The program provides two modes of star formation activity: an instantaneous starburst in which all stars are formed at the same time (then subsequently age) and a continuous, constant star formation rate. For analyzing observations pertaining to the integrated light of entire galaxies,

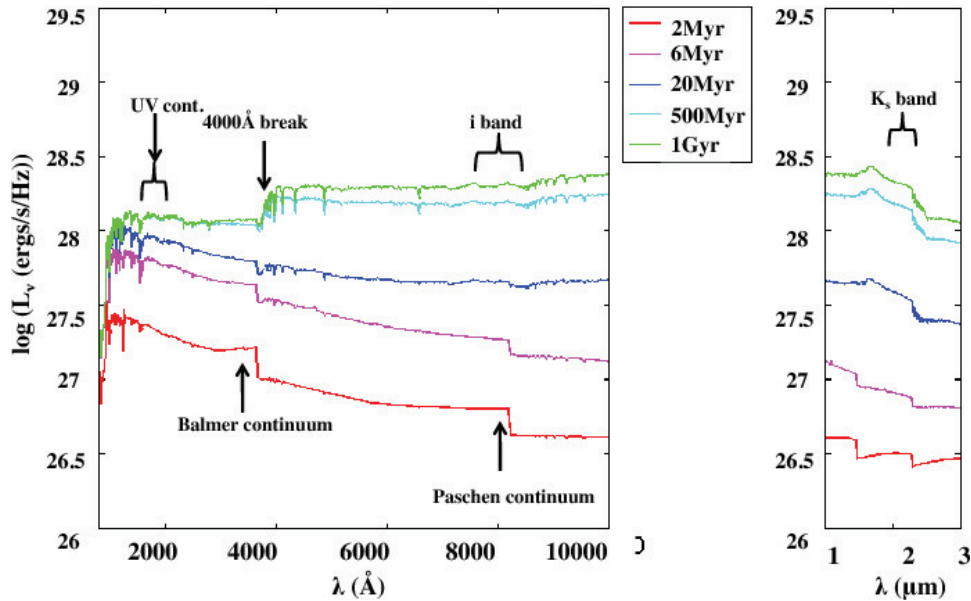


Figure 3. UV, optical and near infrared spectra are shown for a constant rate starburst at  $\text{SFR} = 1 M_{\odot} \text{ yr}^{-1}$  at times up to 1 Gyr (Li et al. 2010). Key spectral diagnostics are noted. Each portion of the spectrum reaches a constant value after a time such that there is equilibrium between birth and death rates for the stars contributing at each wavelength. Thus the asymptotic level progresses from the UV to optical as lower mass stars contribute more at long wavelengths and they have longer evolutionary times. A Kroupa IMF ( $0.1 - 100 M_{\odot}$ ) was used with solar metallicity.

an instantaneous burst is unphysical – the coordination of star formation over a large area is unlikely to be faster than the dynamical timescale  $\sim 100$  Myr.

The Kroupa IMF used as a baseline here has the functional form:  $N(M) \propto M^{-1.3}$  and  $M^{-2.3}$  for  $M = 0.1 - 0.5$  and  $0.5 - 100 M_{\odot}$  respectively. This standard Kroupa IMF is very similar to the Salpeter IMF ( $\alpha = -2.35$ ) on the high mass end, differing only at low masses with a flattening in the Kroupa IMF relative to Salpeter – thus the Salpeter IMF would not change the results here (for UV-optical). For the continuous burst a star formation rate of  $1 M_{\odot} \text{ yr}^{-1}$  was used. For the low redshift starburst galaxies, the adopted solar metallicity is most appropriate; for high- $z$  galaxies, one might expect to have sub-solar metallicities. However, even at high redshift, large departures from solar metallicity have so far not been demonstrated – the observations are preferentially selecting active star forming galaxies either in the restframe UV or dusty galaxies (e.g. submm sources) where high rates of ongoing star formation ensure rapid heavy element enrichment and for the  $z \sim 4 - 6$  SDSS QSOs solar or super-solar metallicity is found from analysis of the QSO emission and absorption lines (e.g. Juarez et al. 2009).

#### 4.1. Starburst Spectral Evolution and Diagnostics

Spectra for the constant rate and instantaneous starbursts are shown in Figures 3 as a function of time. In Fig. 3, we also annotate the key spectral diagnostics: CIV absorption, the UV continuum used to estimate the recent SFR, the  $4000\text{\AA}$  and Balmer

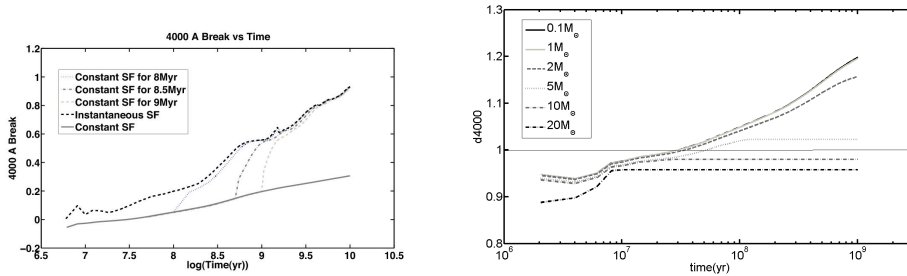


Figure 4. Left – The strength of the 4000 Å break, D4000 in mag, is shown as a function of time for the continuous and instantaneous starburst models (Li et al. 2010). D4000 increases slowly with time for the constant rate starbursts with ongoing SF but then increases steeply after cessation of star formation to a value  $D4000 \approx 0.55$  approximately 300 Myr later. Right – The dependence of D4000 (mag) on the low-mass truncation of the IMF is shown  $M_{low} = 0.1, 1, 2, 5, 10$  and  $20 M_{\odot}$  (Li et al. 2010). A strong D4000 requires that the IMF extend down to  $\sim 2 M_{\odot}$  and post-starbursts and high redshift galaxies exhibiting a strong break must have had IMFs not severely truncated and top-heavy compared to the local Kroupa IMF.

breaks used to constrain the age of the stellar population, and the i-band continuum as a mass estimator.

For the constant rate starburst (Fig. 3), the specific luminosity ( $L_{\nu}$  in ergs/sec/Hz) increases with time at all wavelengths as more mass is added to the stellar population; however, the UV rises less than the optical as the most massive stars die within  $\sim 10$  Myr. The UV at  $\lambda < 2000 \text{ \AA}$  reaches its peak (constant) luminosity after  $\sim 30$  Myr – at this time, equilibrium is established between the rate at which older, hot stars are dying and the rate at which new ones are created by the ongoing SF. Thus for a galactic scale starburst which will last longer than 30 Myr, the intrinsic UV continuum provides a reliable measure of the ongoing SFR. This is in contrast to the optical continuum which exhibits a monotonic rise in time as more low mass stars with longer lifetimes are added. In the red optical continuum (e.g. i-band), the flux rise is approximately linear with time up to  $\sim 500$  Myr. After 500 Myr, the red continuum rises more slowly, since a significant fraction of red optical continuum is contributed by stars of mass 5 –  $10 M_{\odot}$  (for which the main sequence lifetime is  $\sim 500$  Myr).

## 5. The Low Mass IMF From the 4000 Å Break

A major difficulty in assessing the stellar masses of high- $z$  galaxies has been the need to assume an IMF to account for the 'unseen' contribution of low mass stars. For young stellar populations, the optical and UV do not adequately constrain the total mass of stars since the luminosity of the less massive stars is easily dominated by a few massive stars. A number of recent investigations have suggested that the IMF may be quite top heavy in active starburst galaxies (Bunker et al. 2009; Baugh et al. 2005; Meurer et al. 2009). This is motivated by two separate considerations: 1) the lower metallicity gas at high- $z$ , heated by more intense SF activity, is likely to be hotter and therefore have a high Jeans mass limit for gravitational collapse and 2) to reduce the estimated SFRs which in some cases imply very short timescales for consuming the available

ISM. However, no direct observational evidence in high- $z$  galaxies has been found for departures from the local Galactic IMFs (e.g. Kroupa IMF) – in part due to the lack of identified observational probes of the low mass end of the stellar IMF. Even in low- $z$  starburst galaxies, appeals for an altered IMF are usually just to resolve discrepancies with quite uncertain dynamical mass estimates.

For instantaneous starburst models (Li et al. 2010), the 4000Å break feature becomes prominent after  $\sim 100$  Myr (see Fig. 4-left). At earlier times in both continuous and instantaneous burst models, the 4000Å break is reversed (i.e. greater flux on the short wavelength side of 4000Å) due to the strong Balmer continuum emission (associated with OB and A stars). [It is important to note that the 4000Å break should not to be confused with the Balmer break at 3646Å which develops after 6 Myr in the instantaneous burst spectra.]

In the course of our investigation, we realized that since the 4000Å break (and the Balmer break) is in fact a feature arising from cool, lower mass stars, its strength clearly provides a much-needed constraint on the presence of lower mass stars in the IMF. To understand how strong this constraint is, we ran starburst models with the IMF truncated on the low end at a variety of masses ranging from 0.1 to  $20M_{\odot}$ . We then measured the variations in D4000 in these stellar populations. This experiment, for which the results are shown in Fig. 4-right, clearly shows that a strong D4000 index will only be seen in aging stellar populations if the initial mass function extends down to at least  $5 M_{\odot}$ .

The 4000Å break is, in fact, observed in many high- $z$  galaxy SEDs (and used in photometric redshift fitting) indicating that higher mass truncations can not be common at high- $z$  and that the IMF must very likely extend down to  $\sim 2M_{\odot}$ . This feature is also seen with high signal-to-noise ratio in high resolution spectroscopy of local starbursts such as Arp 220 (Rodríguez Zaurín et al. 2008). The inference that the break requires the presence of low mass stars is independent of the choice of IMF form (standard or top-heavy Kroupa) since the break is caused by much lower mass stars. We note that the lack of a high-mass truncation for the IMF at high- $z$  is also supported by studies of the low mass stars in the URSA Minor dwarf spheroidal galaxy – the stellar population there is very old but includes stars down to  $0.3M_{\odot}$  (Wyse et al. 2002)

## 6. Why is the IMF so Invariant ?

At first glance, it would appear puzzling that the IMF is apparently so invariant (or at least that much larger changes are not evidenced in the observations). With just thermal pressure and gravity, the Jeans mass  $M_J = 7(T/10K) (n_H / 10^4)^{-1/2} M_{\odot}$  and one should expect large variations in the ability of different regions to form low mass stars, i.e. hot, low density regions could only form high mass stars. However, in reality, star formation regions or cloud cores become unstable to gravitational collapse and then as these more massive proto-clusters collapse and become denser, fragmentation occurs on the scale of stellar mass concentrations. Thus the ability to form stars of various masses is determined by the densities and temperatures occurring at the time of fragmentation – hence, understanding the scale for this fragmentation is essential if one is to understand the IMF invariance.

Probably it is not unreasonable to physically identify the scale of fragmentation with the scale at which the dust becomes optically thick to its own cooling radiation –

at this point the subcondensations within the cloud core will start to be supported by radiation pressure and their subsequent collapse becomes quasi-static – determined by their limited ability to radiate the gravitational energy. For the expected dust temperatures of  $\sim 30\text{K}$ , a  $1M_{\odot}$  condensation will become optically thick at  $\sim 300\mu\text{m}$  when its size is  $\sim 100\text{AU}$ . At this point the mean density has reached  $10^{11}$  per cc and the Jeans mass is reduced well below  $1M_{\odot}$  even if the gas temperature has risen significantly. In conclusion, the fact that the scale for fragmentation for stellar mass concentrations occurs relatively late in the overall collapse, at times when the gas density has become very large – thus, the initial conditions in the cloud have little or no determining role in setting the final stellar masses.

Is there observational support for this fragmentation scale for the stellar mass condensations? Yes – the distribution of binary star separations may well reflect the fragmentation scale at stellar formation. For an unbiased sample of stars, Duquennoy & Mayor (1991) find a log-normal distribution of orbital separations with peak probability at  $\sim 80$  AU. And for younger weak-line T Tauri stars in the upper Scorpius A & B associations, Brandner & Koehler (1998) found mean separations  $\sim 100\text{AU}$ !

**Acknowledgments.** The modeling of starbursts and the use of the  $4000\text{\AA}$  break to constrain the low mass IMF was done in collaboration with P. Capak (Li et al. 2010).

## References

- Baan, W. A., & Haschick, A. D. 1995, *ApJ*, 454, 745  
 Baugh, C. M., Lacey, C. G., Frenk, C. S., Granato, G. L., Silva, L., Bressan, A., Benson, A. J., & Cole, S. 2005, *MNRAS*, 356, 1191  
 Brandner, W., & Koehler, R. 1998, *ApJ*, 499, L79+  
 Bryant, P. M., & Scoville, N. Z. 1999, *AJ*, 117, 2632  
 Bunker, A., Wilkins, S., Ellis, R., Stark, D., Lorenzoni, S., Chiu, K., Lacy, M., Jarvis, M., & Hickey, S. 2009, ArXiv e-prints. astro-ph/0909.2255  
 Downes, D., & Solomon, P. M. 1998, *ApJ*, 507, 615  
 Duquennoy, A., & Mayor, M. 1991, *A&A*, 248, 485  
 Joseph, R. D., & Wright, G. S. 1985, *MNRAS*, 214, 87  
 Juarez, Y., Maiolino, R., Mujica, R., Pedani, M., Marinoni, S., Nagao, T., Marconi, A., & Oliva, E. 2009, *A&A*, 494, L25  
 Li, G., Scoville, N. Z., & Capak, P. 2010, *ApJ*, submitted  
 Meurer, G. R., Wong, O. I., Kim, J. H., Hanish, D. J., Heckman, T. M., Werk, J., Bland-Hawthorn, J., et al. 2009, *ApJ*, 695, 765  
 Murray, N., Quataert, E., & Thompson, T. A. 2005, *ApJ*, 618, 569  
 Rodríguez Zaurín, J., Tadhunter, C. N., & González Delgado, R. M. 2008, *MNRAS*, 384, 875  
 Sakamoto, K., Scoville, N. Z., Yun, M. S., Crosas, M., Genzel, R., & Tacconi, L. J. 1999, *ApJ*, 514, 68  
 Scoville, N. Z. 2003, *Journal of Korean Astronomical Society*, 36, 167  
 Scoville, N. Z., Evans, A. S., Dinshaw, N., Thompson, R., Rieke, M., Schneider, G., Low, F. J., et al. 1998, *ApJ*, 492, L107+  
 Scoville, N. Z., Polletta, M., Ewald, S., Stolovy, S. R., Thompson, R., & Rieke, M. 2001, *AJ*, 122, 3017  
 Scoville, N. Z., Yun, M. S., & Bryant, P. M. 1997, *ApJ*, 484, 702  
 Thompson, T. A., Quataert, E., & Murray, N. 2005, *ApJ*, 630, 167  
 Vázquez, G. A., & Leitherer, C. 2005, *ApJ*, 621, 695  
 Wyse, R. F. G., Gilmore, G., Houdashelt, M. L., Feltzing, S., Hebb, L., Gallagher, J. S., III, & Smecker-Hane, T. A. 2002, *New Astronomy*, 7, 395